Effects of pre-compression on the detonability of emulsion explosives

by Shulin Nie*

The problem of dead-pressing of emulsion explosives by dynamic pre-compression has been experimentally investigated in four emulsion explosives sensitized either by glass micro-balloons (GMBs) or by chemical gassing. Computer simulation of the dynamic dead-pressing and detonability recovery processes has been carried out in the gassed emulsion explosive. This study showed that the strength of the GMBs determines the pressure tolerance of the explosives. If dead-pressing occurs, it is a very rapid process and takes only few milliseconds. Some explosives can recover their detonability after the dead-pressing. However, the recovery time is quite different for different explosives. For the gassed explosive, the recovery time can be as short as 50 ns, while it is longer than 45 minutes for certain GMB sensitized explosive.

1. Introduction

An emulsion explosive consists of two physical components : matrix and sensitizer. The sensitizer can be hollow glass micro-balloons (GMBs) or gas bubbles generated by chemical or mechanical gassing. When the explosive is subjected to compression, the matrix may start to crystallize, the GMBs may be broken and the gas bubbles may be severely diminished. If any of these occurs, the detonability of the explosive can be deteriorated /1, 2/. In the worst case, a dead-pressing results.

At SveBeFo, the dead-pressing of emulsion explosives has been studied in the search for the reasons for detonation failures in rock blasting practice. The main objective of this study is to investigate the durability of emulsion explosives to pre-compression and the mechanism of dead-pressing.

2. Experimental Studies

2.1 Testing Method

A method of testing the detonability of emulsion explosives under dynamic pre-compression has been developed /3/. The configuration is shown in Fig. 1. Explosives are tested in closed steel pipes measuring

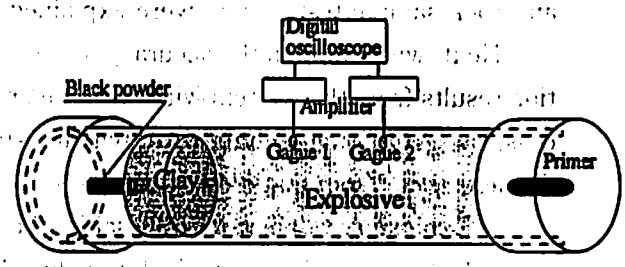

Fig. 1 Method of testing the detonability of emulsion explosives under dynamic pre-compression.

ϕ 52 mm in inner diameter, 4 mm in wall thickness and approximately 1.5 m in length.

The black powder and the detonator are initiated simultaneously. Thus, the burning of the black powder generates a dynamic pressure on the explosive before it is initiated by the primer with a certain delay. The pressure history of the pre-compression on the testing explosive is measured by two pressure gauges, which were developed at SveBeFo based on a piezo ceramic material /4/.

The detonability of the tested explosives was mainly determined by the visual examinations on the test site. If the explosive was dead-pressed, a length, usually about 1 m, of the charge remained after the blast. Otherwise, neither the pipe nor the explosive could be recovered.

Rceived on 1997. 4. 24

*Swedish Rock Engineering Research
Box 49153, S－100 29 Stockholm, Sweden

Table 1 Properties of the tested explosives

Explosive	Matrix density (kg/m³)	Explosive density (kg/m³)	Sensitizer			VOD in ϕ 52 mm steel pipe (m/s)
			Type	Wt-%	Vol-%	
1	1320	1200	Q-CEL 719	1.70	10.7	5812
2	1320	1210	Q-CEL 723	2.05	10.7	(Not measured)
3	1320	1210	B37/2000	3.26	10.7	6249
4	1360	1200	Gassing	0.011	11.76	(Not measured)

Table 2 Detonability of the four tested explosives

Sensitizer in explosives	Dead-pressing pressure	Detonability recovery after dead-pressing
Q-CEL 719	10 MPa	Yes, after ca 45 min.
Q-CEL 723	20 MPa	No, at least not within 1 hr
B37/2000	> 100 MPa	—
Gassing	17 MPa	Yes, wituin 25 ms*

*: The time interval of the delayed detonator used in the experiment was 25 ms. Therefore, the shortest detectable time was 25 ms.

2.2 Properties of the Studied Explosives

Four explosives were tested. They have the same matrix but different sensitizers, see Table 1. Among the GMBs, the Q-CEL 719 has the lowest rupture strength while B37/2000 has the highest.

2.3 Experimental Results

The detonabilities of the four explosives were summarized in Table 2. Detailed results can be obtained in /5/.

Furthermore, the following conclusions can be drawn :

- The damage of the GMBs or gas bubbles is responsible for the dead-pressing.
- The dead-pressing process is very rapid. For example, it takes less than 10 ms to dead-press the explosive containing Q-CEL 719.
- The recovery of the detonability occurs very rapidly in the gassed explosive. On the contrary, once the explosive sensitized by GMBs is dead-pressed, it is permanently dead in rock blasting practice.

3. Computer Simulation of Dynamic Dead-pressing and Detonability Recovery

In order to understand the dynamic processes of the dead-pressing and the detonability recovery in the emulsion explosives, a computer simulation has been carried out for the chemically gassed emulsion explosive /6/. From the simulation, the times necessary for the dead-pressing and the detonability recovery after the dead-pressing are estimated.

3.1 Mechanism of Initiation and Dead-pressing

Initiation mechanism : The initiation mechanism is assumed to be the viscous heating of the matrix and the isentropic compression of the gas bubbles, which heat up the matrix. When the matrix reaches a critical temperature of 300 ℃ /6/, it starts to burn and an initiation results.

Dead-pressing mechanism : During the pre-compression, the matrix flows inwards towards the centres of the gas bubbles. This flow results in a viscous heating in the matrix itself and a compression in the bubbles. The bubble volume decreases. Meanwhile, the bubble temperature increases accordingly and will be higher than that in the surrounding matrix. Therefore, heat dissipation from the gas bubbles to the matrix takes place /2/. This heat loss will cause a further decrease in the bubble volume and temperature. If the explosive is re-shocked by the primer while the gas bubbles are cold and small, the explosive may not be initiated because of insufficient viscous heating and gas compression.

Mechanism of detonability recovery : After the pre-compression vanishes, the gas bubbles expand and their temperature decreases correspondingly. When the temperature in the bubbles is lower than the

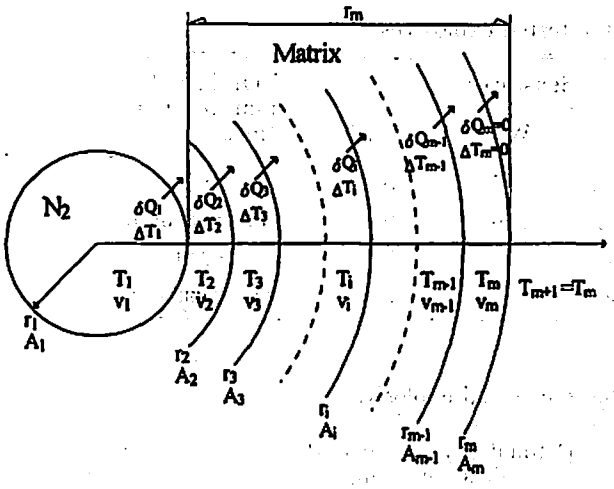

Fig. 2 Element net of the simulation viewed in a plane

matrix temperature, the bubbles will regain heat from the matrix. Gradually, the bubble temperature and the bubble size will return to such a degree that the explosive is detonable again.

3.2 Calculation Algorithm

Geometry and element layout : A spherical symmetry was assumed and the calculations were performed in the spherical co-ordinates, of which the origin is located at the centre of a gas bubble. The matrix surrounding the gas bubble was divided into elements of spherical shells, see Fig. 2.

Pressure profile for pre-compression, initiation and detonability recovery : The pre-compression pressure has a simplified profile. It increases from 1 atm to 17 MPa in 0.1 ms and then keeps constant at 17 MPa, which is an idealized profile based on the measurements from the experiments /6/. The initiation pressure is a shock wave from the primer with an amplitude of 24.8 GPa /6/.

To simulate the recovery of detonability, the pre-compression is suddenly released from 17 MPa to 1 atm after 20 ms of compression /6/.

Program flow chart : The program flow chart is shown in Fig. 3. Four major calculations are carried out in each time step as marked by ①, ②, ③ and ④ in the flow chart. The governing equations for the corresponding calculations are described in the following.

① Viscous flow of matrix and the resultant heating : The matrix can be assumed to be incompressible compared to the gas bubbles. For a viscous and incompressible fluid, the flow is governed by the Navier-

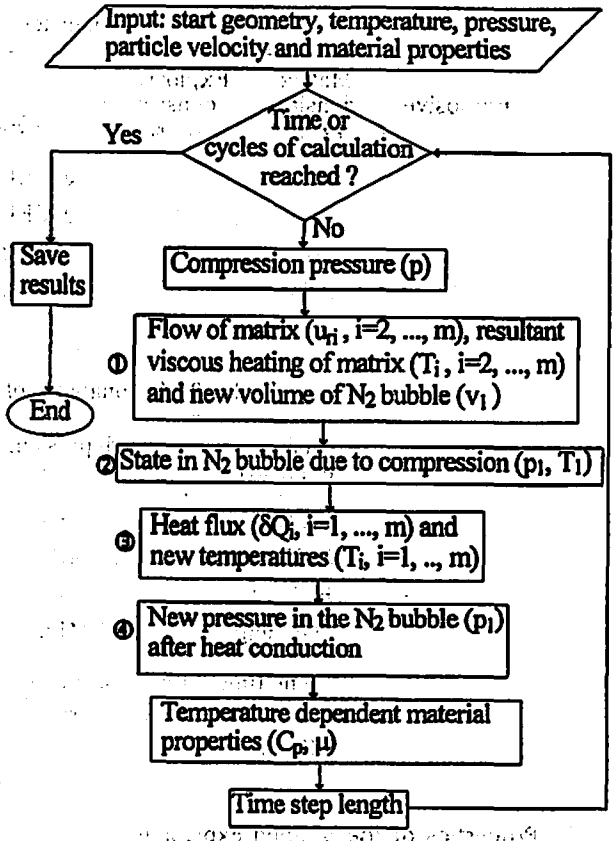

Fig. 3 Program flowchart of the computer simulation

Stoke equation (Eq. 1) and the continuity equation (Eq. 2) /7/. The energy dissipated as viscous heat per unit volume and unit time is in Eq. 3 /7/.

$$\frac{\partial u_r}{\partial t}+(u\cdot\nabla)u_r=-\frac{1}{\rho_m}\cdot\frac{\partial p}{\partial r}+\frac{\mu}{\rho_m}\left[\nabla^2 u_r-\frac{2u_r}{r^2}\right] \quad (1)$$

$$\nabla\cdot u=0 \quad (2)$$

$$E=2\mu(e_{rr}^2+e_{\theta\theta}^2+e_{\phi\phi}^2+e_{\theta\phi}^2+e_{\phi r}^2+e_{r\theta}^2) \quad (3)$$

Where : u_r = radial velocity, (m/s)

t = time, (s)

p = pressure in the matrix, (Pa)

r = radius, (m)

u = velocity vector

= {ur, 0, 0} in a spherically symmetric flow

ρ_m = density of the matrix = 1360 kg/m³

μ = viscosity of the matrix

$=1.60765\cdot10^{12}/T^{4.25477}$ Pa·s, /6/

e_{rr} to $e_{r\theta}$

= components of the rate-of-strain tensor.

The matrix flow determines also the final volume of the gas bubbles (v_1) at the end of each time step.

② State in the gas bubbles due to the compression : The bubble compression was simulated by an isen-

tropic process followed by a heat transmission from the bubble to the surrounding matrix. The isentropic process, dS=0, means : de + $p_1 dv_1 = 0$, or :

$$n \cdot C_v dT_1 + T_1 (\partial p_1 / \partial T_1)_{v1} dv_1 = 0 \quad (4)$$

Where : S is entropy ; e is internal energy ; p_1, v_1 and T_1 are pressure, volume and temperature in the gas bubbles ; n is the amount of gas in each bubble in mol and C_v is the specific heat at constant volume for N_2 gas in J/K/mol.

The van der Waal equation of state (Eq. 5) is assumed to the N_2 gas and the temperature dependence of the specific heat can be described by Eq. 6.

$$(p_1 + an^2/v_1^2)(v_1 - nb) = nRT_1 \quad (5)$$

$$Cv = a_1 + b_1 \cdot T_1 + c_1 / T_1^2 \quad (6)$$

Where : $a = 0.140835$ m^6·Pa/mol^2, /8/

$b = 3.913 \cdot 10^{-5}$ m^3, /8/

$R = 8.31451$ J/K/mol

$a_1 = 20.414$ J/K/mol, /8/

$b_1 = 2.693 \cdot 10^{-3}$ J/K^2/mol, /8/

$c_1 = -3.571 \cdot 10^4$ J·K/mol, /8/

Mathematical manipulations to Eqs. 4, 5 and 6 result in Eq. 7, which together with Eq. 5 determine T_1 and p_1.

$$a_1 \ln T_1 + b_1 T_1 - \frac{c_1}{2T_1^2} + R \cdot \ln(v_1 - nb) - \ln\left[T_0^{a_1} \cdot (v_0 - nb)^R\right] - b_1 T_0 + \frac{c_1}{2T_0^2} \quad (7)$$

Where : v_0 = initial volume = $4\pi r_0^3/3$, (m^3)

T_0 = initial temperature = 20℃ = 293K

r_0 = initial radius = 100μm = 10^{-4} m, /6/

③ Heat flux between elements and the resultant temperature changes : The heat transmission from a bubble to its surrounding matrix occurs on the whole bubble surface and is calculated by Eq. 8. The heat conduction between any two adjacent matrix elements is calculated by Eq. 9 :

$$\delta Q_1 = \alpha A_1 \cdot \Delta T_1 \cdot \delta t, \text{ for } i = 1 \quad (8)$$

$$\delta Q_i = (\lambda / \Delta r_i) \cdot A_i \cdot \Delta T_i \cdot \delta t, \text{ for } i = 2, \cdots, m \quad (9)$$

Where : $i = 1, \cdots, m$ = element number ; 1 for N_2 bubble ; 2 to m for the matrix, see Fig. 2

δQ_i, A_i, ΔT_i, Δr_i = heat flux (J), boundary surface area (m^2), temperature difference (K) respective distance (m) between the i:th and the (i+1):th element, see Fig. 2

α = coefficient of heat transfer
= 4190 W/m^2/K, /2/

λ = thermal conductivity of the matrix
= 0.209 W/m/K, /2/

δt = length of one time step, (s)

The new temperatures in the gas bubble and the matrix elements after the heat conduction are :

$$(T_1)_{new} = (T_1)_{old} - \delta Q_1 / (n \cdot C_p) \quad (10)$$

$$(T_i)_{new} = (\delta Q_{i-1} - \delta Q_i) / (\rho_m \cdot C_{pm} \cdot v_i) + (T_i)_{old}, \text{ for } i = 2, \cdots, m \quad (11)$$

Where : C_p = specific heat at constant pressure for N_2 gas = 1.4·C_v /8/

C_{pm} = specific heat at constant pressure for matrix = 1080 J/kg/K, /2/

④ New pressure in the gas bubbles after heat transmission : The new pressure in the gas bubbles $(p_1)_{new}$ is found by solving Eq. 5, since v_1 and $(T_1)_{new}$ are known at this stage.

3.3 Results of Simulation

Dead-pressing : The simulation showed that after the application of the pre-compression, the radius of the N_2 bubble decreases very rapidly in the beginning but more slowly later on. At the same time, the bubble temperature first increases due to the compression and then decreases due to the heat transmission to the matrix. It is also shown that after 1 ms of compression, the radius and the temperature of the bubble decrease very slowly. After 20 ms, they no longer decrease significantly.

If, at different waiting times during the compression, the explosive is initiated by the primer, different temperature will be induced in the matrix by the primer owing to different state in the bubble and different matrix temperature. Fig. 4 shows how this shock-induced temperature in the matrix element adjacent to the N_2 bubble, which is the highest temperature in the matrix, decreases with the waiting time. According to this figure, the explosive is dead-pressed at waiting times longer than 2 ms.

Recovery of detonability : When the pre-compression vanishes, the gas bubble will expand. At this time, if the explosive is initiated by the primer, a new temperature will be induced in the matrix. Fig. 5 shows such shock-induced temperature in the matrix element adjacent to the gas bubble after the compression vanishes. According to Fig. 5, the explosive is

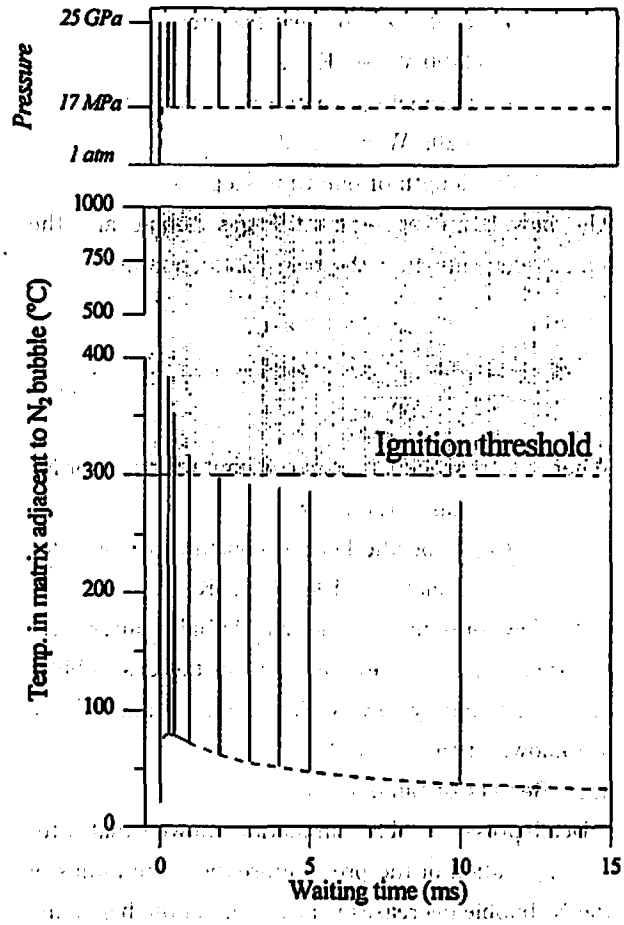

Fig. 4 Temperature in the matrix element adjacent to the N_2 bubble, induced by initiation attempt using the primer at different waiting time during the pre-compression. The corresponding pressure profile is shown in the upper figure. The dashed lines correspond to the pre-compression.

detonable again 50 ns after the step release of the compression.

However, since the release of the pre-compression is simulated by a step release, the simulation did not take into account of the decaying time or decaying speed of the pre-compression release. Consequently, the resultant time of the detonatbility recovery is the theoretical shortest recovery time. In the reality, for example in the blasting experiment, the pressure release has always a finite decaying time which is much longer than 50 ns. Therefore, the visible time of the detonability recovery should be longer than the simulation result of 50 ns.

4. Conclusions

- The simulation resulted in good agreement with the experimental work for the chemically gassed emulsion explosive.

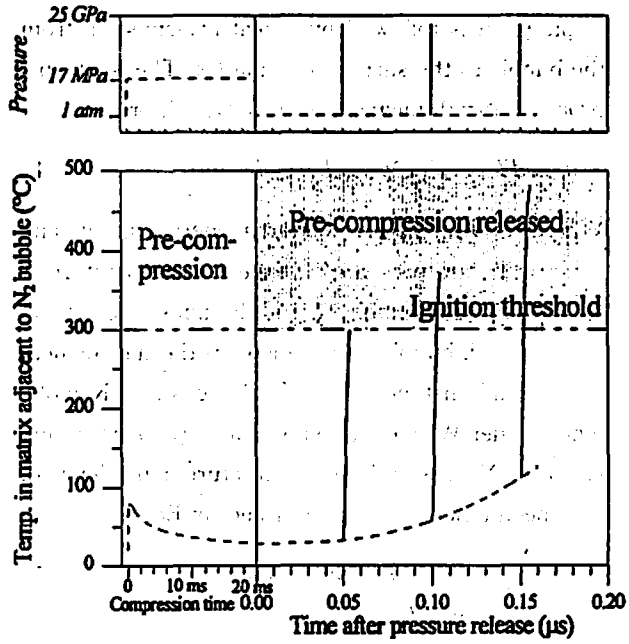

Fig. 5 Temperature in the matrix element adjacent to the N_2 bubble induced by initiation attempts at different time after the pre-compression vanishes. The corresponding pressure profile is shown in the upper figure. The dashed lines correspond to the effects of compression and pressure release along. (Notice the dual time scales.)

- For the explosives containing GMBs, the rupture strength of the GMBs determines their pressure tolerance.
- The detonability of the gassed explosive can be recovered very rapidly, within 50 ns, according to the simulation. This rapid recovery is a unique feature for the gassed emulsion, which the GMB sensitized emulsions do not have.
- Damage of the GMBs or diminution of the gas bubbles is responsible for the dead-pressing.
- The dead-pressing occurs very rapidly, about 2 ms for the gassed emulsion and less than 10 ms for the GMB sensitized emulsions.

Acknowledgement

The experiments described in this paper were carried out with the help of J Deng and U Nyberg at SveBeFo and L Chen at Chinese Academy of Science. The FoU Division at Nitro Nobel AB with the head of Mr. B Engsbråten is also acknowledged for all the assistance provided, especially in manufacturing the matrices and in providing the chemical gassing technology.

References

1) T. Matsuzawa, M. Murakami, Y. Ikeda and K. Yamamoto : "Detonability of Emulsion Explosives under Variable Pressure", J. of the Industrial Explosives Society, Japan. Vol. 43, No. 5, 1982.
2) K. Hanasaki and M. Terada : "Studies on the Sensitivity of Dead Pressed Slurry Explosives in Delay Blasting", Rock Frag. by Blasting - FRAGBLAST-4. Vienna, Austria. July 5－8, 1993.
3) Nie S : "A Method of Studying the Dynamic Dead-pressing of Non-capsensitive Emulsion Explosives", SveBeFo Report DS 1993 : 3, 1993.
4) Nie S, Persson A and Deng J : "Development of a Pressure Gage Based on a Piezo Ceramic Material", Experimental Techniques, May/June, 1993.
5) Nie S : "Pressure Desensitization of emulsion explosives", Rock Frag. by Blasting - FRAGBLAST -4. Vienna, Austria. July 5－8, 1993.
6) Nie S and Chen L : "Dynamic Dead-pressing of a Chemically Gassed Emulsion Explosive", SveBeFo Report 29, 1996.
7) Acheson D J : "Elementary Fluid Dynamics", Clarendon Press, Oxford. 1990
8) Atkins P W : "Physical Chemistry", 4th Edition. Oxford University Press. 1990.

エマルション爆薬の爆轟性に及ぼす先行圧力の影響

Shulin Nie*

動的先行圧力によるエマルション爆薬の死圧の問題について，ガラスマイクロバルーン(GMBs)のみならず化学的ガスの鋭感剤を含む4つのエマルション爆薬を用いて，実験的に調べた。動的死圧と爆轟性の回復過程に関するコンピューターシミュレーションをガス鋭感剤エマルション爆薬について行った。この研究で，GMBsの強度が爆薬の耐圧性を決定することを示した。もし，死圧が生じても，それは非常に急速な過程であり，わずか，数ミリ秒である。ある爆薬は死圧後もその爆轟特性を回復できる。しかしながら，回復時間はそれぞれの爆薬によって全く異なる。あるガラスマイクロバルーン鋭感剤爆薬では回復時間が45分より長いのに対し，ガス鋭感剤の爆薬では，回復時間は50 nsと短い。

(*Swedish Rock Engineering Research, Box 49153, S-100 29 Stockholm, Sweden)